iScience

CellPress
OPEN ACCESS

Article

Into Thick(er) Air? Oxygen Availability at Humans' Physiological Frontier on Mount Everest

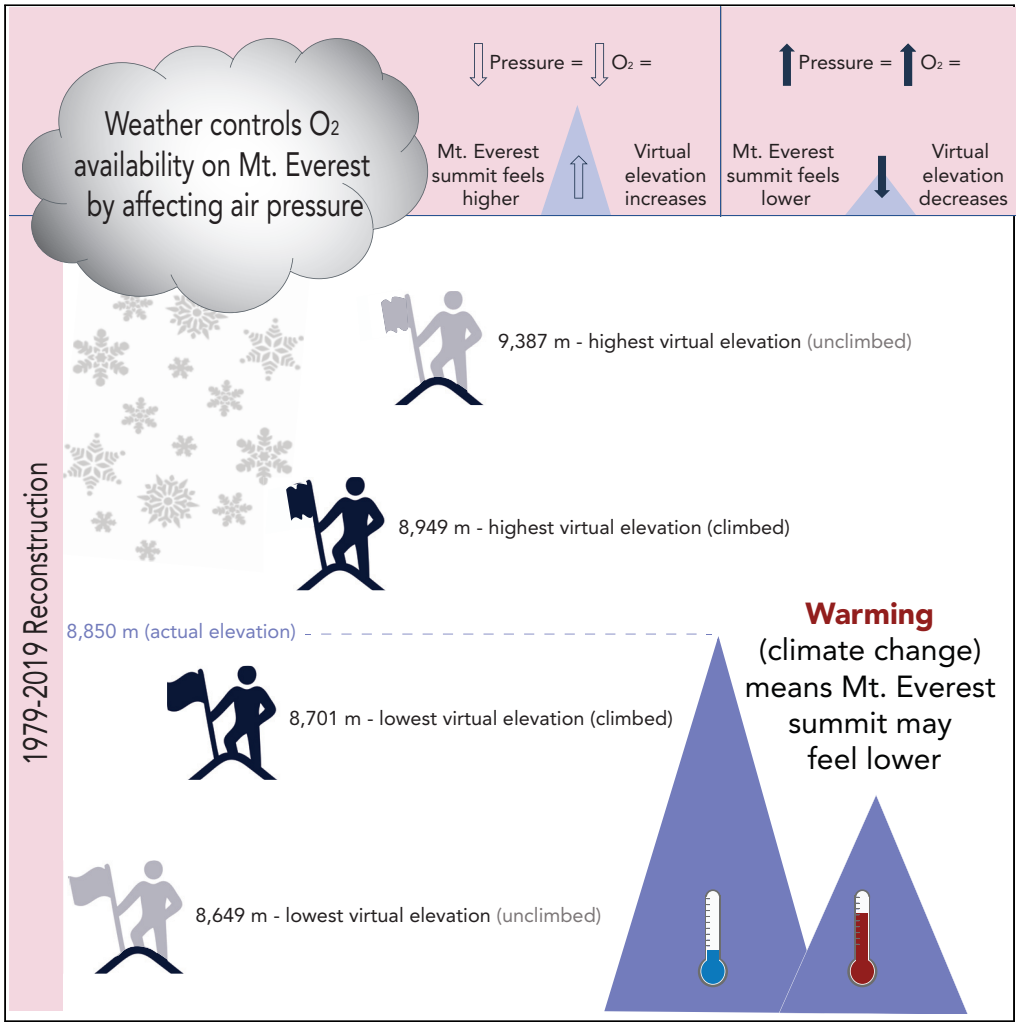

Tom Matthews, L. Baker Perry, Timothy P. Lane, ..., Ananta Gajurel, Mariusz Potocki, Paul A. Mayewski

t.matthews@lboro.ac.uk

HIGHLIGHTS

Mt. Everest's perceived elevation changes by almost 700 m depending on the weather

Air pressure on Mt. Everest summit plunges close to physiological limit in winter

Climate warming is increasing air pressure/ oxygen availability on Mt. Everest

Matthews et al., iScience ■■, 101718
■■, 2020 © 2020 The Authors.
https://doi.org/10.1016/j.isci.2020.101718

Please cite this article in press as: Matthews et al., Into Thick(er) Air? Oxygen Availability at Humans' Physiological Frontier on Mount Everest, iScience (2020), https://doi.org/10.1016/j.isci.2020.101718

iScience

CellPress
OPEN ACCESS

Article

Into Thick(er) Air? Oxygen Availability at Humans' Physiological Frontier on Mount Everest

Tom Matthews,[1,11,*] L. Baker Perry,[2] Timothy P. Lane,[3] Aurora C. Elmore,[4] Arbindra Khadka,[5,6] Deepak Aryal,[5] Dibas Shrestha,[5] Subash Tuladhar,[7] Saraju K. Baidya,[7] Ananta Gajurel,[8] Mariusz Potocki,[9,10] and Paul A. Mayewski[9]

SUMMARY

Global audiences are captivated by climbers pushing themselves to the limits in the hypoxic environment of Mount Everest. However, air pressure sets oxygen abundance, meaning it varies with the weather and climate warming. This presents safety issues for mountaineers but also an opportunity for public engagement around climate change. Here we blend new observations from Everest with ERA5 reanalysis (1979-2019) and climate model results to address both perspectives. We find that plausible warming could generate subtle but physiologically relevant changes in summit oxygen availability, including an almost 5% increase in annual minimum VO_2 max for 2°C warming since pre-industrial. In the current climate we find evidence of swings in pressure sufficient to change Everest's apparent elevation by almost 750 m. Winter pressures can also plunge lower than previously reported, highlighting the importance of air pressure forecasts for the safety of those trying to push the physiological frontier on Mt. Everest.

INTRODUCTION

As the highest mountain on Earth, Mt. Everest is one of the planet's most extreme environments. First climbed almost half a century after the North and South Poles had been reached, the 8,850 m peak (known in Nepal and China as Sagarmatha and Qomolangma, respectively) can experience temperatures as low as −50°C and winds as high as 80 m s^{-1}, placing mountaineers at risk of cold injury in as little as one minute (Huey and Eguskitza, 2001; Matthews et al., 2020; Moore and Semple, 2011). Yet it is the dangers from reduced oxygen availability that provides perhaps the greatest challenge to climbers (West, 2019). In that sense the summit of Mt. Everest is a remarkable frontier, perhaps closer than anywhere else on the Earth's surface to the limits where human physiology can reach.

Oxygen content is so low near the summit of Mt. Everest because its abundance is directly proportional to atmospheric air pressure within the troposphere, and this falls exponentially with increasing elevation. The lower oxygen availability challenges many organ functions (Richalet, 2010; West, 1990), but it is the reduction in potential work rate that so greatly tests mountaineers (West, 1993). Empirical studies have shown that, even in acclimatized individuals, aerobic capacity (expressed by maximal oxygen uptake: VO_2 max) declines exponentially with falling air pressure (Pugh et al., 1964; Sutton et al., 1988; West et al., 1983a). Mt. Everest's summit is so close to the limits of human physiology that the earliest of these studies concluded it could not be reached without climbers breathing bottled oxygen (Pugh et al., 1964; West, 2019). It was only when Reinhold Messner and Peter Habeler summited on May 8, 1978 without supplemental oxygen (an "oxygenless ascent" hereafter) that the highest point on Earth was confirmed as within reach of human physiology. Although theoretical analyses struggled to explain this result, later work concluded that, if a climber's VO_2 max at sea level was sufficiently high, the decline with altitude may not be sufficient to preclude an oxygenless ascent (West et al., 1983a; West and Wagner, 1980).

Critically, it has been recognized that the *relatively* high air pressure on Mt. Everest also plays a key role in enabling oxygenless ascents to 8,850 m. Estimates from radiosondes indicate monthly mean summit air pressures between 324 hPa in winter and 339 hPa in the monsoon (West et al., 1983b). These values are much higher than the 313 hPa predicted by ICAO Standard Atmosphere (an industry-standard model of

[1]Department of Geography & Environment, Loughborough University, Loughborough, UK

[2]Department of Geography & Planning, Appalachian State University, Boone, NC, USA

[3]School of Biological and Environmental Sciences, Liverpool John Moores University, Liverpool, UK

[4]National Geographic Society, Washington, D.C, USA

[5]Central Department of Hydrology & Meteorology, Tribhuvan University, Kathmandu, Nepal

[6]International Centre for Integrated Mountain Development, Lalitpur, Nepal

[7]Department of Hydrology and Meteorology, Kathmandu, Nepal

[8]Department of Geology, Tribhuvan University, Kathmandu, Nepal

[9]Climate Change Institute, University of Maine, Orono, ME, USA

[10]School of Earth and Climate Sciences, University of Maine, Orono, ME, USA

[11]Lead Contact

*Correspondence: t.matthews@lboro.ac.uk

https://doi.org/10.1016/j.isci.2020.101718

the pressure-height relationship), meaning that the physiological challenge of an oxygenless ascent is more manageable than would be inferred from the ICAO prediction (West and Wagner, 1980).

Air pressure is relatively high on Mt. Everest because the rate at which pressure falls with elevation is inversely proportional to the virtual temperature of the atmosphere (Stull, 2015), and Mt. Everest is, along with all other peaks over 8,000 m, located in the warmth of the subtropics. Oxygenless ascents of Earth's highest mountains would be an even greater demand for human physiology if they were located in colder climates (West, 1993, 2010; West and Wagner, 1980). There is also a temporal equivalent of this geographical good fortune that helps place Mt. Everest's summit within reach. Due to variations in the atmosphere's oxygen content through geological time, a hypothetical human would *not* have been able to ascend to 8,850 m for more than two-thirds of the last 570 million years (Huey and Ward, 2005). Similarly, given current rates of tectonic uplift, it has been estimated that Mt. Everest's summit could be beyond the limits of human physiology around 40,000 years from now (Bailey, 2001). However, in the shorter term, anthropogenic climate change is increasing the air pressure on the summit of Mt. Everest as temperatures rise (Moore and Semple, 2009) (because this causes air pressure to fall less rapidly with height). The potential aerobic difficulty of an oxygenless ascent has consequently decreased since the early 20th century and is likely to diminish further with continued warming.

The challenge of climbing to 8,850 m is therefore variable from an oxygen-availability standpoint. By coincidence of geography, atmospheric composition, and climate, it is currently within human aerobic capacity to reach this height without supplemental oxygen. However, the current proximity of Mt. Everest's summit to our physiological frontier is still somewhat unknown. Radiosonde estimates have captured the statistics of summit pressure variability (including the conditions encountered during a handful of famous ascents) (West, 1993), but a systematic, high-resolution assessment of air pressure at the summit is not yet available. Such a contribution would identify the full range of conditions that humans have encountered during past oxygenless ascents and would also clarify how close the summit may encroach upon our aerobic limits during the depths of winter when air pressure is lowest (West et al., 1983b). The latter is of critical relevance to the interest in oxygenless wintertime ascents, highlighted by multiple attempts in the 2019–2020 winter season (Benavides, 2019, 2020).

Beyond the simple upward extrapolation of the trend in summit air pressure by Moore and Semple (2009), an assessment of the potential shifts in the aerobic challenge of Mt. Everest due to climate change is also yet to be undertaken. This is of considerable symbolic and practical significance. Mt. Everest is a global icon symbolizing life at the extremes (Frohlick, 2003), and it has been argued that using tangible and specific examples can help communicate the abstract concept of climate warming (Höijer, 2010). The evolving aerobic difficulty for humans scaling Mt. Everest without supplemental oxygen is, therefore, a topic with the potential to increase public interest in climate change and perhaps improve support for policy response (Smith and Leiserowitz, 2014). The aims of our research are consequently two-fold: (1) to produce a high-resolution reconstruction of air pressure (and thus oxygen availability) on the summit of Mt. Everest, including assessing climbers' experience and exploring extreme low-pressure events; and (2) to investigate the sensitivity of summit air pressures to changes in global mean air temperature.

RESULTS

Observations and Reconstructed Air Pressure

Observed air pressure at the South Col automatic weather station (7,945 m) on Mt Everest (Matthews et al., 2020) shows a distinct seasonal cycle, ranging from a minimum of 358 hPa in January 2020, to a maximum of 387 hPa in June 2019 (Figure 1A). The variation in air pressure is much more substantial in winter than during the summer, with a maximum range of 20 hPa across December 2019 to February 2020, compared with a maximum range of 6 hPa during the 2019 monsoon (July–September: Matthews et al., 2020). We also note from Figure 1A that pressure is subject to relatively large changes over short time scales, exemplified by the swing of almost 20 hPa between February 8 and 13, 2020.

Overlapping data from the ERA5 reanalysis (Hersbach et al., 2020) indicate excellent agreement with South Col air pressure measurements, yielding a Pearson correlation of 0.995 and minimal bias, reduced further by application of the adjustment described in the Methods (Figure 1B). Combined with our method to estimate the vertical gradient in (log) pressure, this correction results in a mean absolute error (MAE) of 0.36 hPa when ERA5 air pressure is extrapolated from the South Col to the Balcony automatic weather station at

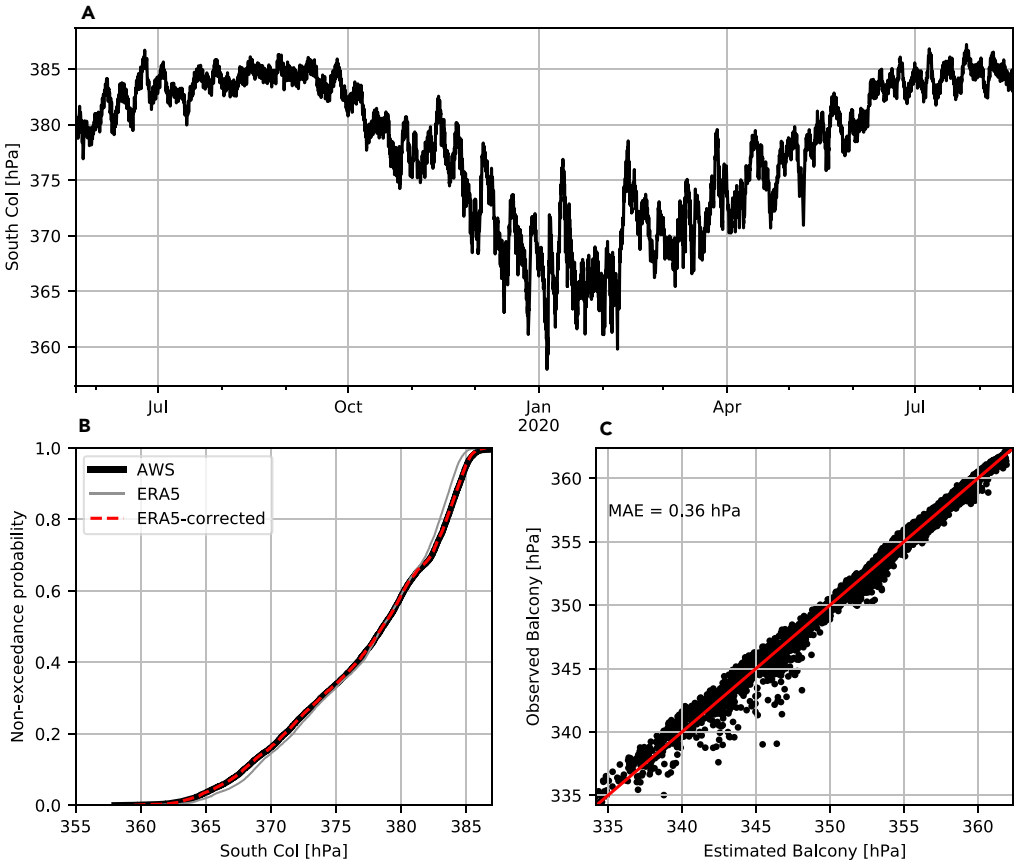

Figure 1. Air Pressure on Mt. Everest

(A) Hourly observed air pressure at the South Col (7,945 m) from May 22, 2019 to July 1, 2020.

(B) Comparison between observed air pressure and ERA5 air pressure for the South Col.

(C) Estimated air pressure at the Balcony (8,430 m) compared with observed air pressure at the Balcony AWS for the time period of May 23, 2019 to January 20, 2020. MAE indicates the mean absolute error for this comparison.

8,430 m (Matthews et al., 2020) (Figure 1C). By comparison, an MAE of 6.45 hPa is obtained if ERA5 data are interpolated directly to the Balcony.

The strong coherence between measured and estimated pressure at the Balcony builds confidence in our ERA5 reconstruction of summit air pressure (Figure 2), where we compute a mean value of 331 hPa over the 1979–2019 period. In agreement with earlier research (West et al., 1983b) we find substantial seasonality, as mean summit pressure ranges from 323 hPa (mid-January) to 339 hPa (mid-August). Consistent with the observational record from the South Col, the width of the blue shading in Figure 2 also highlights that summit pressure is most variable in winter.

The episodes of lowest air pressure are explored in more detail in Figure 3A, where we composite 10 days of air pressure either side of the 20 events with lowest pressure. These local minima fall to values around 10 hPa below the seasonal mean over approximately three to five days, before recovering at a similar rate. The atmospheric circulation during the low-pressure events indicates the presence of an upper-level wave, with its ridge crest over Central Asia, and its trough centered over Mt. Everest's summit (Figure 3B). Waves consistent with the composite in Figure 3B are observed in nearly all of the 20 events (Figure S1), and estimates of their phase speed (see Methods) predict a median transit time from ridge to crest of 3.9 days, in close agreement with the timescale of pressure variability evident in Figure 3A.

The strong upper atmosphere winds of the subtropical jet stream are also evident in Figure 3B, although they are focused to the south of the Himalayas. The relationship between ERA5 winds interpolated to the summit of Mt. Everest is weak during December–February (when all 20 low-pressure events

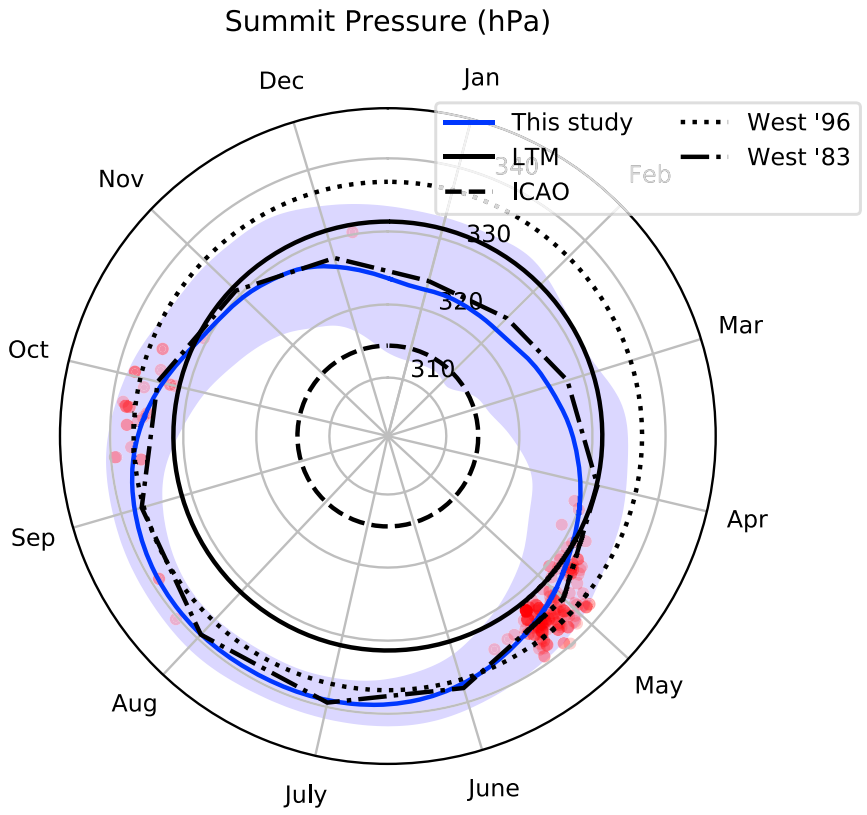

Figure 2. Reconstructed Air Pressure for the Summit of Mt. Everest (1979–2019)

Blue shading spans the reconstructed minimum and maximum for the respective day of year, whereas the solid blue line indicates the mean value for the day. The solid black line (LTM) is the long-term mean for our reconstruction (331 hPa). The other lines appearing in the legend highlight estimates of summit pressure used in the literature (ICAO: ICAO Standard Atmosphere; West '83: West et al. (1983b); West '96: West (1996)). The red circles indicate summit air pressure at the time of successful ascents made without the help of supplemental oxygen (with intensity of shading proportional to the number of climbers). Note that labels are located at the middle of the respective month and that all day-or-year statistics are smoothed with a Gaussian kernel before plotting (see Methods).

occur; r = −0.11), and winds persistently below the wintertime mean are possible even during the extreme low pressure events (Figure 3C). Consistent with the understanding that air pressure falls more rapidly with elevation in colder air masses (see Introduction), we do note a strong correlation between wintertime air temperatures and summit air pressure (r = 0.81).

Air Pressures Encountered during Oxygenless Summits

Over the period of our reconstruction (1979–2019) there have been 10,068 successful ascents of Mt. Everest, and 208 (2.1%) of those were made without the assistance of supplemental oxygen. The vast majority of these oxygenless ascents (81.7%) were achieved in the pre-monsoon month of May, with the next most popular month being October (11.1%) during the post-monsoon (Table 1). Both of these months experience summit pressures above the annual mean approximately three-quarters of the time. Accordingly, the mean summit pressure across all oxygenless summits (335 hPa) is around 4 hPa above the long-term mean (331 hPa). However, we highlight that this value is still somewhat below the 337 hPa often used by physiologists to characterize Mt. Everest's summit pressure (see Figure 2, "West '96")

Successful oxygenless summits were also obtained on days with relatively high oxygen availability for the time of year (Figure 2 and Table 1), with a mean anomaly (relative to the day of year) of 1.0 hPa across all climbs and mean summit pressures during climbs in May and October equivalent to approximately the 70th and 80th percentiles in the respective months. The only winter climb without supplemental oxygen was also attained at a time when pressure was 330 hPa (in close agreement with the 329 hPa reported

Please cite this article in press as: Matthews et al., Into Thick(er) Air? Oxygen Availability at Humans' Physiological Frontier on Mount Everest, iScience (2020), https://doi.org/10.1016/j.isci.2020.101718

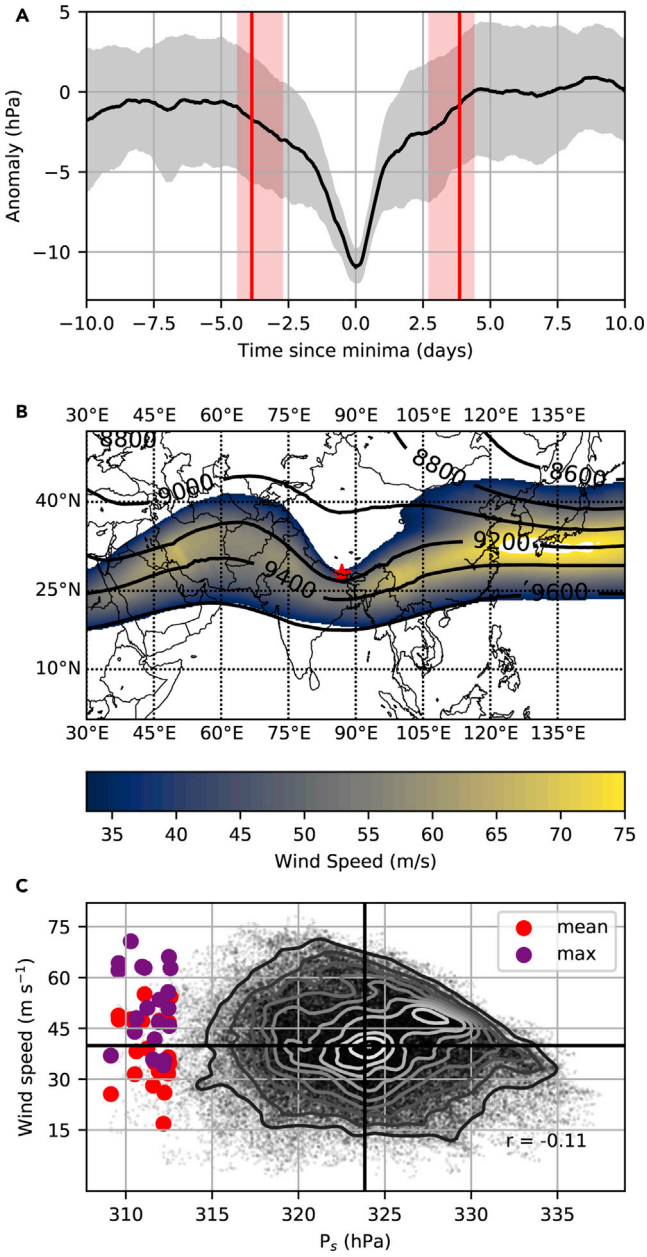

Figure 3. Episodes of Lowest Air Pressure on Mt. Everest (1979–2019)

(A) Composite mean anomaly (black line) ± standard deviation (gray shading) for the 20 reconstructed events with lowest summit pressure. Red vertical lines mark the mean calculated time since minima for pressure to begin falling away from (negative days), or recover to (positive days), higher values. Calculations are based on wave phase speed, and the shading spans the 25th to 75th percentiles of these estimates (see Methods).

(B) Mean geopotential height of the 300 hPa surface (lines) and mean 250 hPa wind (shading) across the 20 events, with Mt. Everest shown as a red star. Note winds <33 m/s (equivalent to a Category 1 hurricane) are not shown. (C) Scatter cloud shows the relationship between hourly winter (Dec-Feb) summit air pressures and concurrent winds interpolated to Mt. Everest's summit. Contours indicate relative density (white higher density, black lower density), whereas heavy black lines indicate the respective means, and *r* is the Pearson correlation. The larger colored circles show the mean (red) and maximum (purple) summit wind speed and pressure in a 72-h window centered on each of the 20 events.

Month	Summits	Summits (% of Total)	Mean Air Pressure (hPa)	Air Pressure Range (hPa)	Exceeding Annual Mean (%)[a]	Exceeding Climbing Mean (%)[b]	Mean Climbing Air Pressure[c]	Mean Climbing Air Pressure Percentile[d]
Jan	0	0	323	26	2.3	0.1	–	–
Feb	0	0	323	27	1.5	0.1	–	–
Mar	0	0	325	23	3.8	0.2	–	–
Apr	4	1.9	329	21	19.6	1.5	330	64.5
May	170	81.7	333	17	78.6	27.1	335	70.8
Jun	2	1.0	337	14	99.8	92.3	334	4.9
Jul	0	0.0	339	8	100.0	100.0	–	–
Aug	3	1.4	339	8	100.0	100.0	339	54.0
Sep	5	2.4	338	13	99.9	96.2	338	33.5
Oct	23	11.1	333	17	73.8	32.5	336	79.3
Nov	0	0.0	329	20	25.4	2.7	–	–
Dec	1	0.5	326	27	9.0	0.8	330.3	86.1

Table 1. Monthly Air Pressure Statistics and Successful Mt. Everest Ascents Made without Supplemental Oxygen (1979–2019)

[a]The percentage of hours within the month when air pressure is above the long-term mean (331 hPa).

[b]The percentage of hours in the month when summit air pressure is above the mean across all oxygenless ascents (335 hPa).

[c]The mean summit air pressure during all successful oxygenless ascents made in the respective month.

[d]The corresponding percentile of the mean in [c] with respect to all summit air pressures in that month.

by West, 1993), which is higher than over 86% of all other December values, and close to the long-term mean (331 hPa). Although very rare, summit air pressures in all winter months (December–February) can rise above the long-term mean, even exceeding the mean pressure during oxygenless summits (0.1–0.8% of the time). The very few oxygenless summits during the normal monsoon months (June–September) took place on days with absolute values either above, or very close to, the mean pressure across all oxygenless summits.

Successful ascents made without supplemental oxygen have occurred during a narrow range of the air pressures that are possible on the summit of Mt. Everest. Similar to Huey and Ward (2005) we communicate this by converting the variations in air pressure to changes in elevation for a typical May day (Figure 4). These metrics indicate how far above (or below) the summit a mountaineer would have to theoretically climb to encounter the respective air pressures. According to these definitions, the hypothetical May mountaineer would have to ascend 97 m beyond the summit to reach a level equivalent to the lowest pressure encountered during any climb without supplemental oxygen (329 hPa; April 1985); they would need to *descend* 150 m to match the highest pressure for an oxygenless summit (340 hPa, August 1980). This difference (247 m) is, however, much less than the 737 m separation calculated between the highest (343 hPa; August 2010) and lowest (309 hPa; February 1993) summit air pressures estimated throughout the reconstruction.

Another way to communicate the environmental effects on a climber at extreme elevations is through the aerobic impact (i.e., the potential VO_2 max: see Methods) at Mt. Everest's summit (Figure 4). Across all oxygenless summits, we calculate that VO_2 max varied between −3.4 (April 1985) and 5.1% (August 1980) of the mean May value, widening to −18.8 (February 1993) and 6.9% (August 2010) across all air pressures in the reconstruction. Relative comparisons are more striking, with estimated VO_2 max on the summit 8.1% lower during the oxygenless summit on 29 April 1985 compared with the successful climb without supplemental oxygen in August 1980. Across the entire reconstruction, conditions during the February 1993 low-pressure episode would cut VO_2 max by 24.0% of the value estimated for the highest-pressure event in August 2010. For context, to reduce VO_2 max by the same fraction (according to the ICAO Standard Atmosphere) would necessitate an ascent from sea level to 3,169 m. Communicated in terms of work rate, we

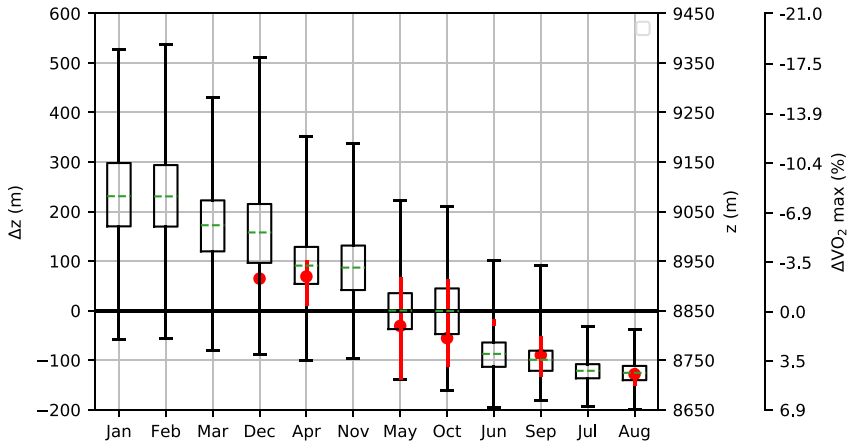

Figure 4. Monthly Variations in the Aerobic Impacts of Oxygen Variability at Mt. Everest's Summit

For each month, Δz is the change in elevation required to reach the respective air pressure, assuming a gradient in log pressure equal to the May mean (0.00014 m^{-1}) and a mean May summit pressure of 333 hPa. Bars extend to the highest and lowest Δz (corresponding to the lowest and highest summit pressures, respectively), whereas boxes span the 25th–75th percentiles, and green lines mark the monthly mean. Note that z (m) is the total perceived summit elevation (Δz + 8,850 m), and ΔVO_2 max converts the respective air pressures to differences in VO_2 max, relative to the mean May conditions (333 hPa = 16.2 mL min^{-1} kg^{-1}). Months are sorted in descending order of mean Δz. Red circles indicate conditions during oxygenless summits, with vertical lines extending to maximum and minimum values [For two summits only the range is plotted; and for one summit the value is denoted by the red circle]. See Supplemental Information for apparent elevation data during previous oxygen-assisted summits.

note that climbing speed under this February lowest pressure event could be reduced by around 41.2% relative to the highest pressure. In an illustrative example, this would result in a climber with a mass of 100 kg (including all equipment) being reduced from an elevation gain of 3.5 m min^{-1} to 2.1 m min^{-1}, almost doubling the time required to climb a given distance. Compared with the lowest pressure experienced during the April 1985 oxygenless summit, the February 1993 low-pressure extreme would lower VO_2 max by 15.9%, equivalent to the reduction expected from climbing from sea level to 2,132 m in the ICAO Standard Atmosphere. The corresponding drop in climbing speed would be 29.5% (see Methods for calculations of climbing rates).

The Impact of Climate Warming on Summit Air Pressure

A shift toward higher summit pressure in the most recent decade is visually evident across the distribution in most months (Figure 5A). This change is, however, clearest during the monsoon months of June–September when variability is reduced. During most of the winter and the popular spring climbing month of May, there is some evidence for an increase in the higher quantiles, but not the lower quantiles, indicating a broadening of the distribution. This picture is supported by trends in the annual statistics of summit air pressure (Figure 5B). Rates of change in annual mean summit pressure [0.35 (95% confidence interval: 0.23–0.48) hPa $decade^{-1}$] and the annual maximum summit pressure [0.24 (0.10–0.36) hPa $decade^{-1}$] are significant, according to the non-parametric Theil-Sen trend estimation, whereas the trend in annual minimum summit pressure [0.27 (−0.29 to 0.85) hPa $decade^{-1}$] is not. The HadCRUT4 dataset (Morice et al., 2012) indicates that global mean annual air temperature increased at a rate of 0.17°C $decade^{-1}$ over the same 1979–2019 interval, meaning that the air pressure trends equate to temperature sensitivities of 2.10 (1.38–2.85), 1.39 (0.58–2.14), and 1.58 (−1.73 to 5.03) hPa $°C^{-1}$ for the annual mean, maximum, and minimum pressures, respectively.

The ensemble of CMIP5 simulations (Taylor et al., 2011; Table S1) offer an alternative estimate of the sensitivity of summit pressure, isolating the impact of climate warming by filtering out interannual variability through the application of running 30-year means. The results show that the largest increases should be in wintertime pressure as global mean annual air temperature rises, with minimum values most sensitive to warming (Figure 5C). This translates to greatest increases in annual minimum summit pressure, rising by 2.56 (2.06–3.47) hPa $°C^{-1}$ compared with sensitivities of 2.06 (1.75–2.62) and 2.18 (1.80–2.66) hPa $°C^{-1}$ for annual mean and maximum summit pressures, respectively (Figure 5D).

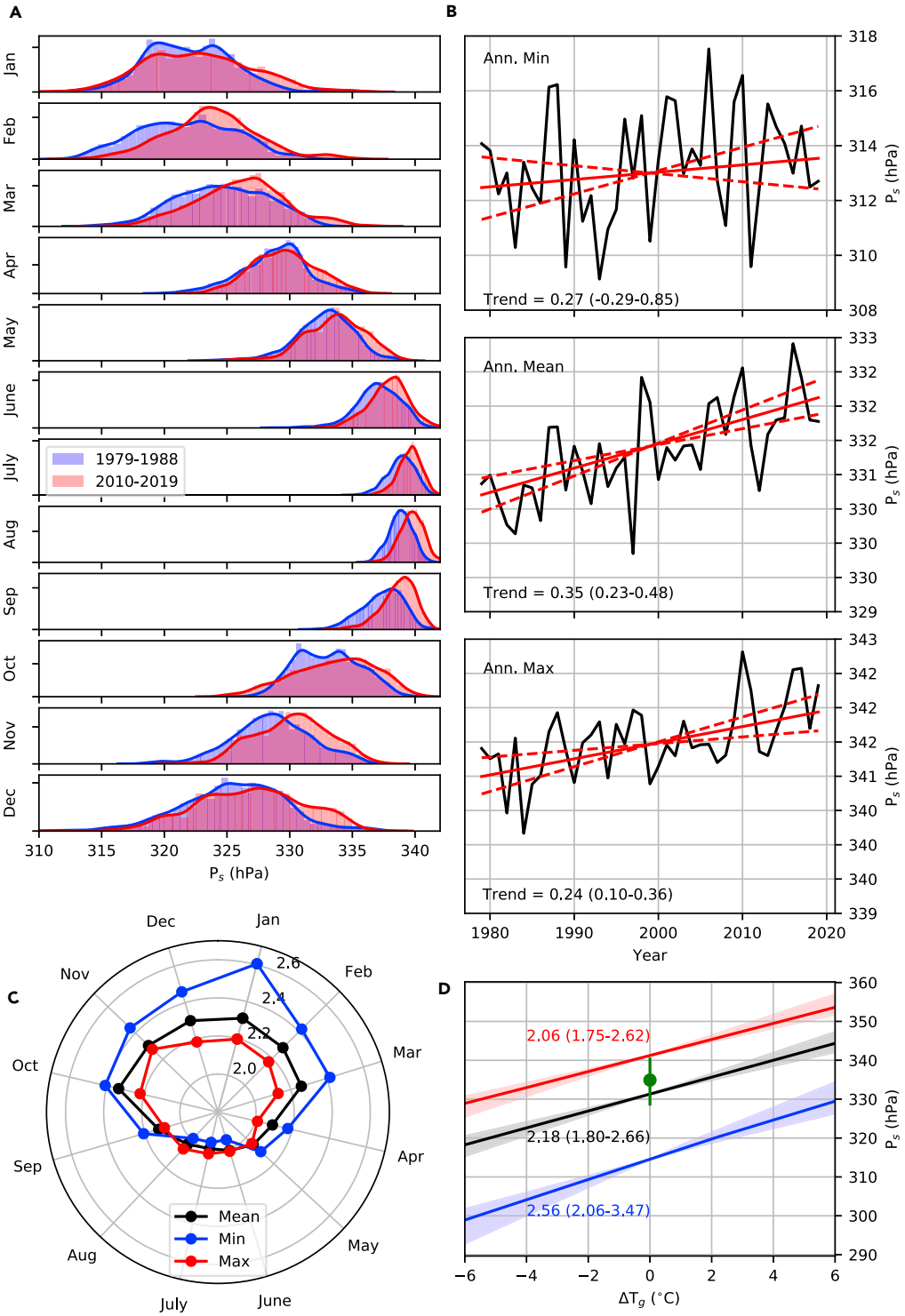

Figure 5. Analysis of Seasonal Air Pressure Changes at Mt. Everest's Summit

(A) Observed distribution of hourly air pressure in the first and last decades of the reconstruction.

(B) Observed trends in annual statistics. The solid red line indicates the median Theil-Sen slope estimate, and the dotted red lines show the 5th–95th percentiles. Decadal trends (and uncertainty range) are annotated at the bottom of each panel.

(C) CMIP5 ensemble median sensitivities of monthly statistics to global mean temperature change (hPa $°C^{-1}$).

Please cite this article in press as: Matthews et al., Into Thick(er) Air? Oxygen Availability at Humans' Physiological Frontier on Mount Everest, iScience (2020), https://doi.org/10.1016/j.isci.2020.101718

Figure 5. *Continued*
(D) CMIP5 projections for annual mean, maximum, and minimum summit pressures for ΔT_g of warming above 1981–2010 global mean temperature Solid lines indicate the CMIP5 ensemble median, whereas shading spans the 5^{th}–95^{th} percentiles. Note that the colors share the same meaning as panel (C), and annotations summarize the gradients (hPa $°C^{-1}$) of the lines plotted (5^{th}–95^{th} percentiles). The green circle marks the mean summit pressure across all successful oxygenless ascents, with green lines extending to the minimum and maximum pressures.

DISCUSSION

Due to a coincidence of geography, atmospheric composition, and climate, it is currently within the range of human physiology to reach the 8,850 m peak of Mt. Everest without supplemental oxygen. This is, however, more the exception than the rule for the last 570 million years (Huey and Ward, 2005), and the transience of Mt. Everest's summit being within our grasp provides a powerful way to communicate environmental change at the extremes of our planet's climate. It is also significant from a practical perspective to those capturing the world's attention with their attempts to summit Mt. Everest without supplemental oxygen (Benavides, 2019, 2020). Here we have provided the highest resolution estimate to date of how close Mt. Everest summit oxygen availability encroaches upon human aerobic limits and the most detailed assessment yet of the impact of climate change in pushing back this frontier.

Our analysis of sensitivities from climate model experiments indicated that plausible scenarios of global warming could result in air pressure changes on Mt. Everest that may be of physiological relevance. A temperature increase consistent with the 2°C limit agreed in the Paris Climate Agreement (UNFCCC, 2015), for example, could increase air pressure by 4–5 hPa relative to pre-industrial conditions (Figure 5C), translating into median changes in VO_2 max of up to 4.9% for annual minimum pressure and 3.3% for annual means. As an example, this would translate to the minimum pressure encountered in our reconstruction (309 hPa) being expected to rise to 314 hPa, reducing the height that a hypothetical mountaineer would need to climb to reach this pressure by around 118 m (from 9,387 m to 9,269 m). Much larger and unlikely (but not implausible; Sherwood and Huber, 2010) temperature increases would translate to more radical changes. For example, with approximately 7.2°C of warming, annual minimum pressures would be elevated to the *current* annual mean, effectively removing the additional low-oxygen challenge inherent with wintertime climbs. A climate 7.2°C warmer than pre-industrial would also raise the annual mean air pressure to 346 hPa—a value encountered around 300 m below the summit in the current climate on a typical May day. On the other hand, annual minimum pressures could be expected to drop below the ~302 hPa threshold for an oxygenless summit (see Methods) in a climate 4.9°C colder than present. Although such cooling is implausible for many millennia to come (Collins et al., 2013; Herrero et al., 2014), temperatures were approximately 5–6°C cooler than present during the Last Glacial Maximum (Snyder, 2016). Our results therefore suggest that a hypothetical oxygenless climb to 8,850 m on Mt. Everest may have been occasionally beyond the limits of human aerobic capacity as recently as 19–26.5 thousand years ago (Clark et al., 2009).

The temperature sensitivities of summit pressure diagnosed by CMIP5 are supported by the general consistency with trends in the 1979–2019 reconstruction. Moore and Semple (2009) noted a similar rate of change in summit air pressure of 0.2–0.3 hPa $decade^{-1}$ using the NCEP reanalysis (1948–2008; Kistler et al., 2001). However, the authors then suggested that the implied 2–3 hPa increase from 1958 to 2048 would increase VO_2 max by ~10%, far greater than the sensitivity we report here. This discrepancy seems to be because Moore and Semple (2009) did not adjust for the fact that the partial pressure of oxygen changes by ~0.21 hPa for every 1 hPa increase in (total) air pressure (see Oxygen Availability and VO_2 max in Methods), meaning they overestimate the impact on VO_2 max by approximately a factor of five.

The large amount of warming required to elevate annual minimum pressures to the annual mean reflects the substantial seasonal cycle in summit air pressure for the current climate, with pressure in the depths of winter on average 16 hPa below values during the height of the monsoon. This range is consistent with previous estimates of seasonality and highlights how variable the aerobic challenge of an oxygenless ascent can be across a typical year (West et al., 1983b). We noted, however, that climbers succeeding with such attempts have been exposed only to a narrow sample of the conditions that are possible. This is mostly because oxygenless summits have been restricted to the relatively high-pressure months of May and October, but also because mountaineers exhibit a preference for climbing during episodes of relatively high pressure for the time of year, as reported elsewhere (Firth et al., 2008). The result is that, although across oxygenless summits the minimum VO_2 max was reduced by 8.1% relative to its peak, the minimum

Please cite this article in press as: Matthews et al., Into Thick(er) Air? Oxygen Availability at Humans' Physiological Frontier on Mount Everest, iScience (2020), https://doi.org/10.1016/j.isci.2020.101718

pressure event in February 1993 (309 hPa) would result in a VO_2 max 15.9% lower still, slowing the potential climbing rate by almost another third. Even though this February low-pressure extreme was above the theoretical ~302 hPa threshold, the potential for such considerable increases in aerobic difficulty questions whether oxygenless summits are *always* within the grasp of human physiology under the current climate. The challenge of climbing Mt. Everest without supplemental oxygen in winter has been raised before but based on ~324 hPa to characterize summit pressure (Garrido et al., 2019; West, 1999). Our reconstruction emphasizes that this value may be an appropriate descriptor of average conditions, but highlights the possibility of much lower pressures still, agreeing with previous research in noting the importance of variability (weather) around the mean (Moore and Semple, 2004, 2011; Moore et al., 2012).

The possibility of such challenging aerobic conditions has immediate practical consequences due to the renewed interest in wintertime oxygenless summits (Benavides, 2019, 2020). There are two observations from our analysis that may improve climber safety here. The first is the speed at which extreme low-pressure events can arrive. In agreement with Moore and Semple (2004) we noted declines in the order of ~10 hPa in under four days, attributed to traveling upper-level waves embedded in the subtropical jet stream. This fall is equivalent to the difference in mean air pressures between May and January, occurring in the time it takes to climb from base camp to the summit and underscoring the importance of weather forecasts for climber safety. However, our second observation highlights that extreme low-pressure events are *not* associated with strong wintertime winds, which is the parameter usually employed to identify suitable weather windows for climbing (Peplow, 2004). As expected from the physical drivers of air pressure variation at high altitude, we do observe a strong correlation between reconstructed pressure and estimated temperature, but extreme cold is generally considered less of a barrier to wintertime mountaineering on Mt. Everest (Ogata, 1995). Our findings therefore strongly suggest that those attempting to make oxygenless ascents in winter should explicitly consult forecasts of summit air pressure. Given that wintertime pressure can occasionally even exceed levels more typical of the most popular climbing month of May, an oxygenless ascent of Mt. Everest in the depths of winter need not even push the physiological frontier if the weather window can be chosen wisely.

Dedicated forecasts of oxygen availability (through air pressure) could also pay dividends for mountaineers attempting to climb without supplemental oxygen in more popular climbing months. Although our results indicated that variability is suppressed relative to the winter, changes in May air pressure, for example, can still drive physiologically relevant reductions in VO_2 max (Moore and Semple, 2004, 2006), important for the safety and success of high-elevation mountaineers (Richalet et al., 1988). Future research should explore this potential, as initial assessments indicate that numerical weather forecasts can skillfully capture atmospheric variability on Mt. Everest's upper slopes (Matthews et al., 2020). Added impetus for this development may be provided if future research determines that oxygen availability has a detectable influence on mountaineering success and safety, perhaps including for those climbing *with* supplemental oxygen (Fontanarosa et al., 2000; Huey et al., 2020).

To conclude, we have provided the most comprehensive assessment yet of oxygen availability at the summit of Mt. Everest, including quantifying its sensitivity to climate change. The results highlight that plausible amounts of warming from greenhouse gas emissions could potentially lead to physiologically relevant increases in oxygen availability, albeit to a lesser extent than indicated by previous research. This interesting consequence may be a powerful means to engage the wider public in climate change, but it is less practically relevant than the substantial seasonal and weather-induced variability in summit pressure confirmed by our analysis. The potential for rapid transitions to low pressures, close to human physiological limits, underscores the need for careful deployment of weather forecasts to help ensure the safety of those pushing the envelope on Mt. Everest.

Limitations of the Study

There are several caveats that should be acknowledged when interpreting our study. First, it is recognized that reanalyses products are subject to temporal inhomogeneities, as the number and type of observations assimilated changes with time (Schneider and Fogt, 2018; Thorne and Vose, 2010). The reanalysis product used here to reconstruct summit air pressures (ERA5) starts in 1979, so it is not prone to any shocks from the widespread introduction of upper-air observations in the 1940s and 1950s (Stickler et al., 2009) or from the beginnings of satellite data assimilation in the late 1970s (Kistler et al., 2001). However, earlier years in ERA5

do suffer from far fewer observations of all forms (Hersbach et al., 2020), meaning that the uncertainties presented for our air pressure reconstruction are likely conservative in the earlier part of the record.

Second, the 21 CMIP5 models we used in our analysis represent, on average, warming up to 4.5°C above the 1981–2010 baseline. Projections of summit pressure for climates warmer still (e.g. 7.2°C above pre-industrial, as discussed in the text) or much cooler than 1981–2010 (e.g. approaching the temperatures of the Last Glacial Maximum) therefore require considerable extrapolation beyond the range of climate change scenarios assessed here. The projections of summit air pressure under such very different climates results should therefore be treated with caution.

We also highlight that, although we used 302 hPa as the lower limit for an oxygenless ascent, variability in individuals' aerobic fitness means that this threshold is not static. The 302 hPa value we applied is representative of very fit mountaineers, with a sea level VO_2 max of approximately 57 mL kg^{-1} min^{-1} (Bailey, 2001; Pugh et al., 1964; Sutton et al., 1988; West et al., 1983a); individuals with higher sea level VO_2 max (including some climbing Sherpa: Brutsaert, 2008; Garrido et al., 1997; Gilbert-Kawai et al., 2014) may be capable of oxygenless ascents at air pressures below 302 hPa. Our estimates of climbing rates mentioned in the text are similarly representative of this sea-level VO_2 max and may underestimate the speeds that some climbers are capable of.

Resource Availability

Lead Contact

Tom Matthews, Department of Geography and Environment, Loughborough University, UK, t.matthews@lboro.ac.uk.

Materials Availability

The study generated no new materials.

Data and Code Availability

The observational data from the automatic weather stations on Mt. Everest are available from National Geographic: https://www.nationalgeographic.org/projects/perpetual-planet/everest/weather-data/

Hourly ERA5 reanalysis data on pressure levels can be obtained freely from the Copernicus Climate Data Store, available here: https://cds.climate.copernicus.eu/cdsapp#!/dataset/reanalysis-era5-pressure-levels?tab=form.

The CMIP5 data (see Supplementary Information Table S1 for the models used) can be accessed freely through the Earth System Grid Federation (https://pcmdi.llnl.gov/mips/cmip5/data-access-getting-started.html).

The reconstructed summit air pressures for all oxygen ascents are available here: https://docs.google.com/spreadsheets/d/14IAtgzZt36YudrhHN0tAPWS4-ddyWf_9IfZx-Yy8kQQ/edit?usp=sharing.

Code used in the analysis is accessible on GitHub: https://github.com/climatom/OneEarth_Everest_O2.

METHODS

All methods can be found in the accompanying Transparent Methods supplemental file.

SUPPLEMENTAL INFORMATION

Supplemental Information can be found online at https://doi.org/10.1016/j.isci.2020.101718.

ACKNOWLEDGMENTS

This research was conducted in partnership with National Geographic Society, Rolex, and Tribhuvan University, with approval from all relevant agencies of the Government of Nepal. The 2019 Everest Expedition made this research possible, and for their role in keeping the team safe and enabling the science goals to be met on the expedition we thank: Conrad Anker, Peter Athans and Sandra Elvin; as well the entire Sherpa

team. The core AWS Sherpa were Panuru Sherpa (Sirdar), Phu Tashi Sherpa, Pemba Sherpa, Urken Lendu Sherpa, Ila Nuru Sherpa, Fura Chetten Sherpa, Lakpa Gyaljen Sherpa, Pasang Sona Sherpa, Pasang Kami Sherpa, Nima Rita Sherpa, Tenzing Gyanjen Sherpa, Nawang Phinjo Sherpa, Phinjo Sherpa, and Gyaljen Dorji Sherpa. Dawa Yangzum Sherpa and Tenzing Gyalzen Sherpa also provided helpful assistance during the installations. We also wish to thank the communities of the Khumbu Region, Xtreme Climbers Treks and Expedition P. Ltd, and Jiban Ghimire and Shangri-La Nepal Trek Pvt. Ltd. ICIMOD gratefully acknowledges the support of its core donors: the Governments of Afghanistan, Australia, Austria, Bangladesh, Bhutan, China, India, Myanmar, Nepal, Norway, Pakistan, Sweden, and Switzerland. We greatly appreciate the efforts of the engineers at Campbell Scientific, Inc (Mike Hansen, Jared Campbell, Steve Gunderson, and Gary Roberts) for designing the AWSs. Finally, Raymond Huey and one anonymous reviewer are thanked for the very insightful comments that helped improve our study.

AUTHOR CONTRIBUTIONS

Conceptualization, T.M. and T.L.; Methodology, T.M.; Resources, T.M., L.B.P., A.K., D.A., D.S., A.G., P.A.M., A.C.E.; Writing - Original Draft, T.M.; Writing - Editing, T.M., T.P.L., A.C.E., A.K., D.S., S.T., S.K.B., M.P., P.A.M.

DECLARATION OF INTERESTS

The authors declare no competing interests.

Received: August 17, 2020
Revised: October 9, 2020
Accepted: October 16, 2020
Published: November 20, 2020

REFERENCES

Bailey, D.M. (2001). The last "oxygenless" ascent of Mt Everest. Br. J. Sports Med. *35*, 294–296.

Benavides, A. (2020). Everest : push begins, Kobusch Passes 7,000m. https://explorersweb.com/2020/02/24/everest-push-begins-kobusch-passes-7000m/.

Benavides, A. (2019). Jost Kobusch to solo Everest in winter. https://explorersweb.com/2019/12/09/jost-kobusch-to-solo-everest-in-winter/.

Brutsaert, T.D. (2008). Do high-altitude natives have enhanced exercise performance at altitude? Appl. Physiol. Nutr. Metab. *33*, 582–592.

Clark, P.U., Dyke, A.S., Shakun, J.D., Carlson, A.E., Clark, J., Wohlfarth, B., Mitrovica, J.X., Hostetler, S.W., and McCabe, A.M. (2009). The last glacial maximum. Science *325*, 710–714.

Collins, M., Knutti, R., Arblaster, J., Dufresne, J.-L., Fichefet, T., Friedlingstein, P., Gao, X., Gutowski, W.J., Johns, T., Krinner, G., et al. (2013). Long-term climate change: projections, commitments and irreversibility. In Climate Change 2013: The Physical Science Basis. Contribution of Working Group I to the Fifth Assessment Report of the Intergovernmental Panel on Climate Change, T.F. Stocker, D. Qin, G.-K. Plattner, M. Tignor, S.K. Allen, J. Boschung, A. Nauels, Y. Xia, V. Bex, and P.M. Midgley, eds. (Cambridge University Press), pp. 1035–1136.

Firth, P.G., Zheng, H., Windsor, J.S., Sutherland, A.I., Imray, C.H., Moore, G.W.K., Semple, J.L., Roach, R.C., and Salisbury, R.A. (2008). Mortality on Mount Everest, 1921-2006: descriptive study. BMJ *337*, a2654.

Fontanarosa, P., Huey, R.B., and Eguskitza, X. (2000). Supplemental oxygen and mountaineer death rates on Everest and K2. JAMA *284*, 181.

Frohlick, S.E. (2003). Negotiating the "global" within the global Playscapes of Mount Everest. Can. Rev. Sociol. *40*, 525–542.

Garrido, E., Rodas, G., Javierre, C., Segura, R., Estruch, A., and Ventura, J.L. (1997). Cardiorespiratory response to exercise in elite Sherpa climbers transferred to sea level. Med. Sci. Sports Exerc. *29*, 937–942.

Garrido, E., Soria, J.M., and Salisbury, R. (2019). Breathless and dying on Mount Everest. Lancet Respir. Med. *7*, 938–939.

Gilbert-Kawai, E.T., Milledge, J.S., Grocott, M.P.W., and Martin, D.S. (2014). King of the mountains: Tibetan and Sherpa physiological adaptations for life at high altitude. Physiology *29*, 388–402.

Herrero, C., García-Olivares, A., and Pelegrí, J.L. (2014). Impact of anthropogenic CO2 on the next glacial cycle. Clim. Change *122*, 283–298.

Hersbach, H., Bell, B., Berrisford, P., Hirahara, S., Horányi, A., Muñoz-Sabater, J., Nicolas, J., Peubey, C., Radu, R., Schepers, D., et al. (2020). The ERA5 global reanalysis. Q. J. R. Meteorol. Soc. *146*, 1999–2049.

Höijer, B. (2010). Emotional anchoring and objectification in the media reporting on climate change. Public Underst. Sci. *19*, 717–731.

Huey, R.B., Carroll, C., Salisbury, R., and Wang, J.-L. (2020). Mountaineers on Mount Everest: effects of age, sex, experience, and crowding on rates of success and death. PLoS One *15*, e0236919.

Huey, R.B., and Eguskitza, X. (2001). Limits to human performance: elevated risks on high mountains. J. Exp. Biol. *204*, 3115–3119.

Huey, R.B., and Ward, P.D. (2005). Climbing a triassic Mount Everest: into thinner air. JAMA *294*, 1761–1762.

Kistler, R., Kalnay, E., Collins, W., Saha, S., White, G., Woollen, J., Chelliah, M., Ebisuzaki, W., Kanamitsu, M., Kousky, V., et al. (2001). The NCEP–NCAR 50-year reanalysis: monthly means CD-ROM and documentation. Bull. Amer. Meteorol. Soc. *82*, 247–268.

Moore, G.W.K., and Semple, J.L. (2011). Freezing and frostbite on Mount Everest: new insights into wind chill and freezing times at extreme altitude. High Alt. Med. Biol. *12*, 271–275.

Moore, G.W.K., and Semple, J.L. (2009). The impact of global warming on Mount Everest. High Alt. Med. Biol. *10*, 383–385.

Moore, G.W.K., and Semple, J.L. (2006). Weather and death on Mount Everest: an analysis of the into thin air storm. Bull. Amer. Meteorol. Soc. *87*, 465–480.

Matthews, T., Perry, L.B., Koch, I., Aryal, D., Khadka, A., Shrestha, D., Abernathy, K., Elmore, A.C., Seimon, A., Tait, A., et al. (2020). Going to extremes: installing the world's highest weather stations on Mount Everest. Bull. Amer. Meteorol. Soc. https://doi.org/10.1175/BAMS-D-19-0198.1.

Moore, G.W.K., and Semple, J.L. (2004). High himalayan meteorology: weather at the South Col of Mount Everest. Geophys. Res. Lett. *31*.

Moore, K., Semple, J., Cristofanelli, P., Bonasoni, P., and Stocchi, P. (2012). Environmental conditions at the South Col of Mount Everest and their impact on hypoxia and hypothermia experienced by mountaineers. Extreme Physiol. Med. *1*, 2.

Morice, C.P., Kennedy, J.J., Rayner, N.A., and Jones, P.D. (2012). Quantifying uncertainties in global and regional temperature change using an ensemble of observational estimates: the HadCRUT4 data set. J. Geophys. Res. Atmos. *117*.

Ogata, Y. (1995). The ascent of Sagarmatha southwest face in winter. Himalayan J. *51*, https://www.himalayanclub.org/hj/51/3/the-ascent-of-sagarmatha-southwest-face-in-winter/.

Peplow, M. (2004). High winds suck oxygen from Everest. https://doi.org/10.1038/news040524-2.

Pugh, L.G.C.E., Gill, M.B., Lahiri, S., Milledge, J.S., Ward, M.P., and West, J.B. (1964). Muscular exercise at great altitudes. J. Appl. Physiol. *19*, 431–440.

Richalet, J.-P. (2010). Operation Everest III: COMEX '97. High Alt. Med. Biol. *11*, 121–132.

Richalet, J.-P., Keromes, A., Dersch, B., Corizzi, F., Mehdioui, H., Pophillat, B., Chardonnet, H., Tassery, F., Herry, J.-P., Rathat, C., et al. (1988). Caractéristiques physiologiques des alpinistes de haute altitude. Sci. Sport *3*, 89–108.

Schneider, D.P., and Fogt, R.L. (2018). Artifacts in century-length Atmospheric and coupled reanalyses over Antarctica due to historical data availability. Geophys. Res. Lett. *45*, 964–973.

Sherwood, S.C., and Huber, M. (2010). An adaptability limit to climate change due to heat stress. Proc. Natl. Acad. Sci. U S A *107*, 9552–9555.

Smith, N., and Leiserowitz, A. (2014). The role of emotion in global warming policy support and opposition. Risk Anal. *34*, 937–948.

Snyder, C.W. (2016). Evolution of global temperature over the past two million years. Nature *538*, 226–228.

Stickler, A., Grant, A.N., Ewen, T., Ross, T.F., Vose, R.S., Comeaux, J., Bessemoulin, P., Jylhä, K., Adam, W.K., Jeannet, P., et al. (2009). The comprehensive historical upper-air network. Bull. Amer. Meteorol. Soc. *91*, 741–752.

Stull, R. (2015). Practical Meteorology: An Algebra-Based Survey of Atmospheric Science, First. ed. (University of British Columbia).

Sutton, J.R., Reeves, J.T., Wagner, P.D., Groves, B.M., Cymerman, A., Malconian, M.K., Rock, P.B., Young, P.M., Walter, S.D., and Houston, C.S. (1988). Operation Everest II: oxygen transport during exercise at extreme simulated altitude. J. Appl. Physiol. *64*, 1309–1321.

Taylor, K.E., Stouffer, R.J., and Meehl, G.A. (2011). An overview of CMIP5 and the experiment design. Bull. Amer. Meteorol. Soc. *93*, 485–498.

Thorne, P.W., and Vose, R.S. (2010). Reanalyses suitable for characterizing long-term trends. Bull. Amer. Meteorol. Soc. *91*, 353–362.

UNFCCC, 2015. Adoption of the Paris Agreement (No. FCCC/CP/2015/L.9/Rev.1). https://unfccc.int/resource/docs/2015/cop21/eng/l09r01.pdf.

West, J.B. (2019). Lessons from extreme altitudes. Front. Physiol. *10*, 703.

West, J.B. (2010). American medical research expedition to Everest. High Alt. Med. Biol. *11*, 103–110.

West, J.B. (1999). Barometric pressures on Mt. Everest: new data and physiological significance. J. Appl. Physiol. *86*, 1062–1066.

West, J.B. (1996). Prediction of barometric pressures at high altitude with the use of model atmospheres. J. Appl. Physiol. *81*, 1850–1854.

West, J.B. (1993). Acclimatization and tolerance to extreme altitude. J. Wilderness Med. *4*, 17–26.

West, J.B. (1990). Limiting factors for exercise at extreme altitudes. Clin. Physiol. *10*, 265–272.

West, J.B., Boyer, S.J., Graber, D.J., Hackett, P.H., Maret, K.H., Milledge, J.S., Peters, R.M., Pizzo, C.J., Samaja, M., Sarnquist, F.H., et al. (1983a). Maximal exercise at extreme altitudes on Mount Everest. J. Appl. Physiol. *55*, 688–698.

West, J.B., Lahiri, S., Maret, K.H., Peters, R.M., and Pizzo, C.J. (1983b). Barometric pressures at extreme altitudes on Mt. Everest: physiological significance. J. Appl. Physiol. Respir. Environ. Exerc. Physiol. *54*, 1188–1194.

West, J.B., and Wagner, P.D. (1980). Predicted gas exchange on the summit of Mt. Everest. Respir. Physiol. *42*, 1–16.

iScience, Volume ■ ■

Supplemental Information

Into Thick(er) Air? Oxygen Availability at Humans' Physiological Frontier on Mount Everest

Tom Matthews, L. Baker Perry, Timothy P. Lane, Aurora C. Elmore, Arbindra Khadka, Deepak Aryal, Dibas Shrestha, Subash Tuladhar, Saraju K. Baidya, Ananta Gajurel, Mariusz Potocki, and Paul A. Mayewski

Supplemental Information

Supplemental Figures and Tables

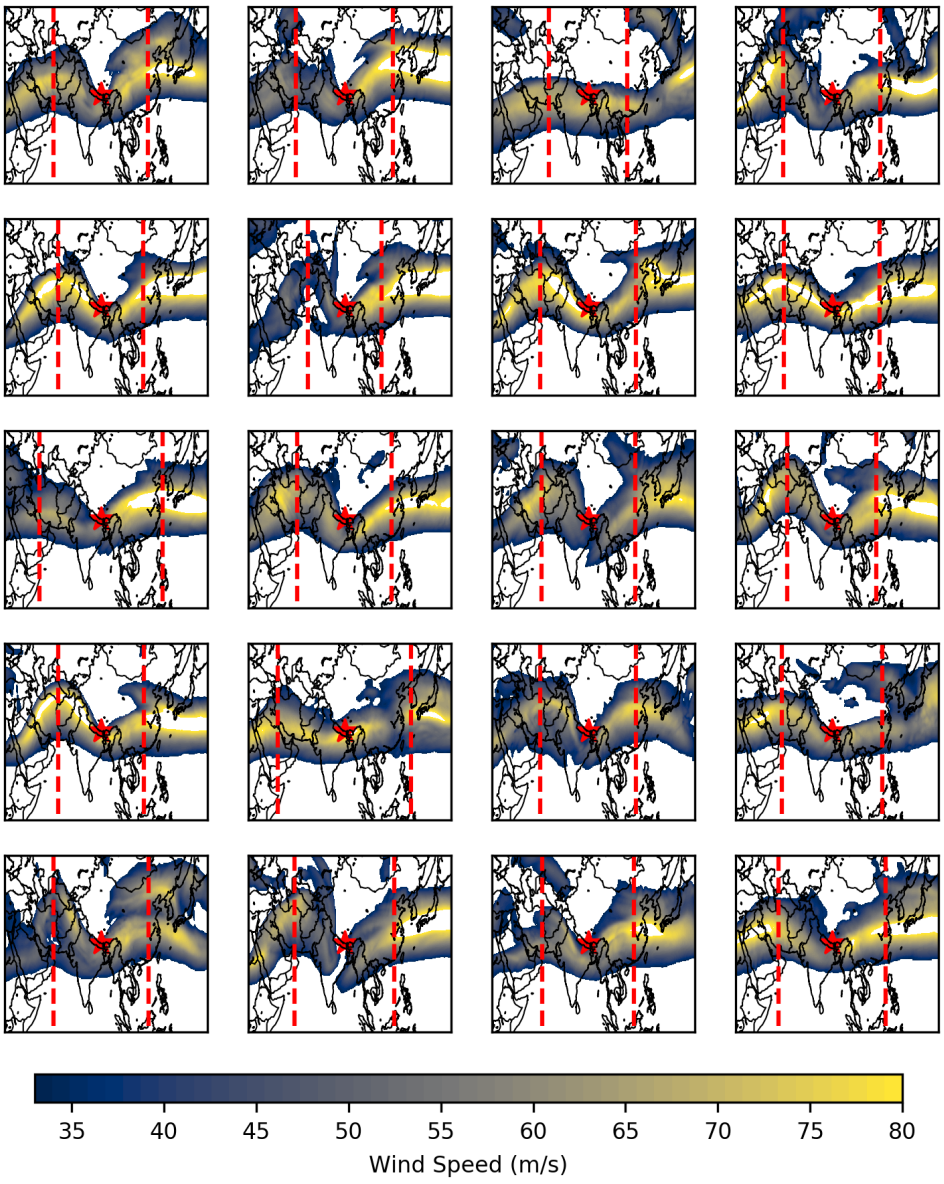

Figure. S1: Atmospheric circulation during the 20 events of lowest air pressure on the summit of Mount Everest, related to Fig. 3A. Colour ramp shows the wind at the 250 hPa pressure level, and the dotted red lines indicate the position of the wave crests identified by the algorithm described in the Transparent Methods (Atmospheric Circulation During Low Pressure Events).

Institute	Model
IPSL	IPSL-CM5B-LR
CMCC	CMCC-CESM
MIROC	MIROC-ESM-CHEM
LASG-CESS	FGOALS-g2
CCCma	CanESM2
BNU	BNU-ESM
NCC	NorESM1-M
BCC	bcc-csm1-1-m
NOAA-GFDL	GFDL-CM3
NOAA-GFDL	GFDL-ESM2G
MRI	MRI-CGCM3
MIROC	MIROC5
MOHC	HadGEM2-CC
IPSL	IPSL-CM5A-LR
MPI-M	MPI-ESM-MR
CMCC	CMCC-CMS
MIROC	MIROC-ESM
CMCC	CMCC-CM
CSIRO-BOM	ACCESS1-0
CSIRO-BOM	ACCESS1-3
IPSL	IPSL-CM5A-MR

Table S1. CMIP5 models used in the analysis, related to Fig 5 (C and D). Note that for each model we employed ensemble member R1i1p1 of the RCP8.5 experiment.

Transparent Methods

Estimation of Mt. Everest Summit Air Pressure

We use observations from the South Col (7,945 m) and Balcony (8,430 m) automatic weather stations (AWSs) deployed on the main southern (Nepalese) climbing route during the 2019 National Geographic and Rolex Perpetual Planet Everest Expedition (Matthews et al., 2020). For the South Col, hourly mean air pressure data were employed from 06:00 UTC May 22, 2019 to 06:00 UTC July 1, 2020. At the

Balcony, the record used is shorter (01:00 UTC May 23, 2019 to 05:00 UTC January 20, 2020), as that station stopped transmitting during the 2019/2020 winter.

To reconstruct air pressure over the longer-term, we used the ERA5 reanalysis from the European Centre for Medium Range Weather Forecasting (Hersbach et al., 2020). We extracted hourly geopotential height, air temperature and wind speed on pressure surfaces for the full period of data availability at the time of analysis (00:00 UTC on January 1, 1979 to 21:00 UTC on June 20, 2020) and then bi-linerarly interpolated these data to the location of Mt. Everest's summit (27.98 °N, 86.93 °E). Air pressure was also interpolated to the location of the longer-running South Col AWS (7,945 m), where an empirical quantile mapping procedure was used to remove systematic bias (Gudmundsson et al., 2012):

$$P_c = f(P_r, x, y) \quad \text{Eq. 1}$$

Where f is a function that interpolates to find the corrected value of the South Col reanalysis air pressure (P_c), given the uncorrected reanalysis data (P_r) and ordered samples *x, y*:

$$x = g^{-1}(P_{r-cal}, q) \quad \text{Eq. 2}$$

and:

$$y = g^{-1}(O, q) \quad \text{Eq. 3}$$

Where $P_{r-cal}$is the air pressure subset of reanalysis data that overlaps with the AWS observations (06:00 UTC May 22, 2019 to 21:00 UTC on June 20, 2020); O is the observed air pressure at the South Col AWS; $q$is vector of quantiles (0.01 to 0.99 in increments of 0.01); and g is the cumulative distribution function. Note that the interpolation was only applied to values of R_r within the range of P_{r-cal}; values outside were adjusted with:$P_c = P_r + \{g^{-1}(O, k) - g^{-1}(P_{r-cal}, k)\}$, where k adopts values of 0.01 and 0.99 when $R_r$is below and above the range of P_{r-cal}, respectively.

Air pressures were then estimated at the summit of Mt. Everest according to the hypsometric equation (Stull, 2015):

$$P_2 = P_1 \times exp(\frac{z_1 - z_2}{a\,\overline{T_v}})$$

Eq. 4

where P_x denotes air pressure at height z_x (m), a is constant (29.3 m K^{-1}) and $\overline{T_v}$ is the mean virtual air temperature (K) between heights z_1 and z_2.

We rewrite Eq. 4 to get the gradient in (log) air pressure as a function of elevation ($\frac{ln(p_2)-ln(p_1)}{z_1-z_2} = \Delta ln(P)/\Delta z$):

$$\Delta ln(P)/\Delta z = a\overline{T_v}^{-1}$$

Eq. 5

Enabling air pressure at the summit (P_s) to be evaluated from (corrected) air pressure at the South Col:

$$P_s = P_c \times exp(\frac{903}{a\,\overline{T_v}})$$

Eq. 6

Where 903 (m) is the vertical separation between the South Col and the 8,850 m summit.

To enable application of Equation 6, it is necessary to know $\overline{T_v}$ between the South Col and the summit, which we estimated from:

$$\overline{T_v} = 0.5 \times (2 \times T_{col} + \Gamma\Delta z)$$

Eq. 7

where T_{col} is the ERA5 air temperature interpolated from pressure levels to the location of the South Col AWS; and Γ is the temperature lapse rate ($\Delta T/\Delta z$), obtained from the air temperature and geopotential height on the 300 and 400 hPa pressure surfaces (a conservative selection intended to bound the maximum pressure at the South Col and minimum pressure at the summit). Any biases in the renalysis $\overline{T_v}$ will, however, affect our assessment of the vertical (log) pressure gradient (Eq. 7). To correct for this, we used air pressures at the Balcony and South Col AWSs to estimate the hourly vertical gradient in log pressure, and regressed this on concurrent $a\overline{T_v}^{-1}$ for the overlapping period. Substitution

into Eq. 6 enables the summit pressure to be estimated using these empirically determined slope (β) and intercept (α) regression terms:

$$P_s = P_c \, exp\left(\frac{903}{\alpha + \beta(a\,\overline{T_v})}\right)$$

Eq. 8

P_s was reconstructed for the complete calendar years 1979-2019. Day of year quantities presented in the text and Fig. 2 were computed by first computing the statistic for the respective day (1-366), and then smoothing these values via convolution with a Gaussian filter set to have a standard deviation of seven days.

Oxygen Availability and VO_2 max

Air pressure was converted to VO_2 max by first calculating the partial pressure of inspired oxygen (P_{io}):

$$P_{io} = 0.2095 \times (P_s - 62.9)$$

Eq. 9

where 62.9 (hPa) is the saturation vapour pressure at the human body's core temperature of 37 °C, and 0.2095 represents the volume fraction of oxygen in the atmosphere (Wallace and Hobbs, 1977).

We then rearranged the regression equation of Bailey (2001) (who synthesised the results of Pugh et al., 1964; Sutton et al., 1988; and West et al., 1983b) to obtain the aerobic capacity (VO_2 max, ml kg^{-1} min^{-1}) of acclimatized individuals as a function of P_{io}(in hPa):

$$VO_2max = \frac{ln(P_{io} \times 0.750) - 3.25}{0.0308}$$

Eq. 10

Equations 9 and 10 therefore enable changes in summit air pressure to be communicated in terms of aerobic impact -- the reduction in VO_2 max due to declining oxygen availability. Bailey (2001) estimate a minimum of 12.25 ml kg^{-1} min^{-1} (3.5 metabolic equivalent expenditures: METs) is required to safely ascend Mt. Everest, assuming summertime conditions, and that climbers are operating at around 85 % of their VO_2 max. Inserting this value into Eq. 10 and solving for P_s (via Eq. 9) yields a threshold air pressure of 302 hPa at the summit for Mt. Everest to be climbable without supplemental oxygen. As discussed in the Limitations (main text), we note that variation in VO_2 max amongst mountaineers is not

accounted for here, and the 302 hPa threshold we identify is representative of fit mountaineers. Some climbers (including elite climbing Sherpa; Brutsaert, 2008; Garrido et al., 1997; Gilbert-Kawai et al., 2014) will have even higher VO_2 max than determined by Eq. 10, and may therefore be able to complete an oxygenless summit at air pressures below 302 hPa.

Atmospheric Circulation During Low Pressure Events

Low pressure events were defined as the 20 lowest hourly air pressure values, separated from other minima by at least two days. To explore atmospheric circulation during these events, we composited the height of the 300 hPa surface (the pressure level closest to the summit of Mt. Everest), and wind velocity at the 250 hPa surface (where the subtropical jet stream is normally located; Ren et al., 2011). Inspection of the composite (Figure 3B), and of the circulation during the individual events (Supplementary Information, Figure S1), indicated the presence of a well-defined upper-level trough with its axis centred at the longitude of Mt. Everest. For each of the 20 waves we calculated the zonal distance from Mt. Everest's summit to the well-defined ridge crest often found to the east, whose location was identified as the longitude with maximum geopotential height along 28 °N, 30-86.9 °E. Doubling this zonal distance provided an estimate of the wavelength (λ) for each of the waves. The time taken for these waves to transit Mt. Everest was estimated using their phase speed (c), calculated assuming barotropic instability, which is a reasonable approximation away from the polar front (Stull, 2015):

$$c = -\frac{2\Omega}{R} cos(\theta) \times \left(\frac{\lambda}{2\pi}\right)^2 + U_{500} \quad \text{Eq.11}$$

where Ω is the Earth's angular velocity (7.29 $\times 10^{-5}$ radians s^{-1}), R is the Earth's radius (6.371 $\times 10^6$ m), $\theta$is the latitude (set to 28 °N here), and $U_{500}$is the mean wind velocity (m s^{-1}) at the 500 hPa level, averaged over the rectangular region 20-40 °N, 30-150 °E. The time taken for the wave trough to arrive/depart Mt. Everest was then evaluated as $\frac{\lambda}{2c}$. It is this time horizon which is marked with vertical red lines in Figure 3A.

Air Pressure and Oxygen Availability During Summit Climbs

The Himalayan Database (Hawley and Salisbury, 2007) provides a comprehensive history of Mt. Everest mountaineering. We used it here to identify successful climbs without supplemental oxygen over the period 1979-2019, extracting reconstructed summit air pressure for the hour that each climber reached the peak. For 19 of these 208 ascents, the exact time was not recorded, so we estimated the summit pressure at the time of ascent using a Gaussian weighted average (with a standard deviation of 3.5 h) centred at 12:00 Nepal Time (NPT) on the day of the successful climb. These choices reflect the mean and standard deviation of summit times across the 189 records that recorded this information.

Estimates of Work Rate and Climbing Speed

Estimates of maximum work rate (W) were informed by the empirical relationship outlined by West et al. (1983b). We digitized the regression line plotted in their Fig. 2, extracting the slope (β) and intercept (α) coefficients to enable conversion between quantities.:

$$W = \beta \times VO_2max + \alpha \quad \text{Eq. 12}$$

The value of β and α were, respectively, determined to be 41.54 kg^2 m ml^{-1}, and -255.96 kg m min^{-1}. Before applying Eq. 12, we reduced each VO_2 max by 15 % to acknowledge that mountaineers likely climb at 85 % of their VO_2 max (Bailey, 2001). W is in units of kg m min^{-1}, and the speed of vertical ascent (m min^{-1}) can be isolated if the mass (kg) of the mountaineer is prescribed. Following West et al. (1983b), we set the mass of the hypothetical climber (including equipment) to 100 kg. Note that because W is a function of VO_2, work rates and climbing speeds should be interpreted as representative of fit mountaineers, but not necessarily elite climbing Sherpa (see Limitations in main text).

The Impact of Climate Change on Summit Pressure

To summarise changes in summit pressure over the period of ERA5 reconstruction (1979-2019), we computed the monthly minimum, mean, and maximum summit pressures. Rates of change were then summarised for these quantities using the Theil-Sen slope estimation method (Sen, 1960; Theil, 1950). The respective trends were termed *significant* if zero lay outside the 95 % confidence interval of the slope estimate.

We used daily mean pressure level CMIP5 output from 21 models forced by the RCP8.5 experiment (Taylor et al., 2011) to determine the sensitivity of Mt. Everest summit air pressure to global mean warming. For each model (listed in Table S1) the same interpolation method applied to the ERA5 reanalysis data to estimate summit pressure was employed. We also extracted the respective near-surface global mean air temperature (T_g) simulated by the corresponding model.

The sensitivity of Mt. Everest summit pressure to changes in T_g was then evaluated using the change factor approach (Osborn et al., 2016). Briefly, this comprised (i) estimating the modelled sensitivity of summit pressures to changes in global mean temperature; (ii) multiplying this sensitivity by a prescribed temperature perturbation; and (iii) adding this result to air pressures in the baseline climate. We achieved (i) by first smoothing CMIP5 P_s and T_g with a running 30-year mean filter, and then regressing P_s upon T_g. Regressions were performed on a seasonal basis, assessing the sensitivity of the (30-year mean) monthly minimum, maximum, and mean summit pressures to climate warming. The results from this analysis were a 21-member ensemble of regression slope coefficients indicating the sensitivity (β_{month}^{stat}, hPa °C^{-1}) to statistic $_{stat}$ (minimum, maximum or mean) in the respective $_{month}$. The monthly stratification of the regression coefficients was warranted because for mean and minimum summit pressure, a single factor ANOVA indicated significant differences across months ($p < 0.01$). Evidence for different sensitivities of maximum summit pressure across months was weaker ($p = 0.13$), but we kept the monthly stratification to be consistent across statistics.

For each model, steps (ii) and (iii) were achieved by transforming the sensitivities (β_{month}^{stat}) to absolute values of air pressure ($\widehat{P_{s_{month}}^{stat}}$) given prescribed changes (Δ) to T_g through:

$$\widehat{P_{s_{month}}^{stat}} = \beta_{month}^{stat} \Delta T_g + P_{s_{month}}^{stat} \quad \text{Eq. 13}$$

where $P_{s_{month}}^{stat}$ is the 1981-2010 statistic for the respective month in the ERA5 reconstructed summit air pressure series. The median, 5th, and 95th percentiles of β_{month}^{stat} across the model simulations were used to indicate, respectively, the central estimate and uncertainty in application of Eq. 13. Annual means, minima and maxima were then evaluated for the respective climates by calculating the relevant statistic from these transformed series. We characterized departures from the 1981-2010 global mean air

temperature using the HadCRUT4 dataset (Morice et al., 2012). Note that according to these data, this period was 0.60 °C warmer than preindustrial, defined here as 1850-1879.

Supplemental References

Gudmundsson, L., Bremnes, J.B., Haugen, J.E., Engen-Skaugen, T., 2012. Technical Note: Downscaling RCM precipitation to the station scale using statistical transformations – a comparison of methods. Hydrol. Earth Syst. Sci. 16, 3383–3390. https://doi.org/10.5194/hess-16-3383-2012

Hawley, E., and R. Salisbury. "The Himalayan Database: The Expedition Archives of Elizabeth Hawley," 2007. https://www.himalayandatabase.com/.

Osborn, T.J., Wallace, C.J., Harris, I.C., Melvin, T.M., 2016. Pattern scaling using ClimGen: monthly-resolution future climate scenarios including changes in the variability of precipitation. Clim. Change 134, 353–369. https://doi.org/10.1007/s10584-015-1509-9

Ren, X., Yang, X., Zhou, T., Fang, J., 2011. Diagnostic comparison of wintertime East Asian subtropical jet and polar-front jet: Large-scale characteristics and transient eddy activities. Acta Meteorol Sin 25, 21–33. https://doi.org/10.1007/s13351-011-0002-2

Sen, P.K., 1960. On Some Convergence Properties of U-Statistics. Calcutta Statistical Association Bulletin 10, 1–18. https://doi.org/10.1177/0008068319600101

Theil, H., 1950. A Rank-Invariant Method of Linear and Polynomial Regression Analysis. Koninklijke Nederlandse Akademie var Wetenschappen Proceedings 53, 386–392. (Part 1), 521–525 (Part 2), 1397–1412 (Part 3).

Wallace, J.M., Hobbs, P.V., 1977. Atmopsheric Science: An Introductory Survey. Academic Press, New York.

West, J.B., Lahiri, S., Maret, K.H., Peters, R.M., Pizzo, C.J., 1983b. Barometric pressures at extreme altitudes on Mt. Everest: physiological significance. J Appl. Physiol. Respir. Environ. Exerc. Physiol. 54, 1188–1194. https://doi.org/10.1152/jappl.1983.54.5.1188